Electronic Supplementary Information

to the

Nucleation Kinetics of Lithium Phosphate Precipitation

Michael Emmanuel, Paszkál Papp, Gábor Schuszter, Ágota Deák, László Janovák, Ágota Tóth and Dezső Horváth

A Determination of the solubility product

To 70 mL of distilled water, 7 g of the dried powdered Li_3PO_4 was added, and the conductance of the resulting solution was measured in 20-s intervals by a conductivity meter (Thermo Orion 420A Plus) while constantly stirring. From the conductance of the saturated solution relative to the solvent, the conductivity $\kappa = 0.102 \pm 0.003$ S m^{-1} was obtained. The solubility of Li_3PO_4 was expressed as

$$c_L = \frac{\kappa}{3\lambda^0_{Li^+} + \lambda^0_{PO_4^{3-}}} = 2.59 \text{ mM} \tag{S1}$$

where $\lambda^0_{Li^+} = 3.866$ mS m^{2}mol^{-1} and $\lambda^0_{PO_4^{3-}} = 27.84$ mS m^{2}mol^{-1} are the limiting molar conductivity of the ions.[1] The solubility product was then readily available according to

$$K_{sp} = 27\left(\frac{c_L}{c^\theta}\right)^4 = (1.2 \pm 0.1) \times 10^{-9} \tag{S2}$$

B Preliminary induction time measurements

Initial experiments has been performed to find conditions under which no effect of the cuvette wall is observed and the induction time measurements show good reproducibility (see Table S1). Special care has been taken to avoid contamination where significant heterogeneous nucleation can occur. Additional experiments are also presented in Table S1 with unfiltered solutions where the effect of

Table S1 Preliminary induction time measurements

$[PO_4^{3-}]_0$(M)	Cuvette	Condition	t_{ind}(s)
0.06	glass	filtered	562 ± 36
0.06	quartz	filtered	565 ± 36
0.1	glass	filtered	46 ± 6
0.1	quartz	filtered	45 ± 6
0.06	glass	unfiltered	313 ± 60
0.06	quartz	unfiltered	369 ± 6
0.1	glass	unfiltered	37 ± 4
0.1	quartz	unfiltered	38 ± 3

heterogeneous nucleation is detectable. This scenario is only shown here as a reference and has not been under investigation in the study.

C Dependence of induction time on supersaturation

At the high concentration used in our experiments, the dependence of induction time on supersaturation exhibits deviation from the linear relationship applicable to smaller supersaturation closer to equilibrium according to the classical nucleation theory (see Fig. S1). Kinetic effects can explain the tendency, as our model calculation also matches the experimental data although small contribution from heterogeneous nucleation cannot be excluded.

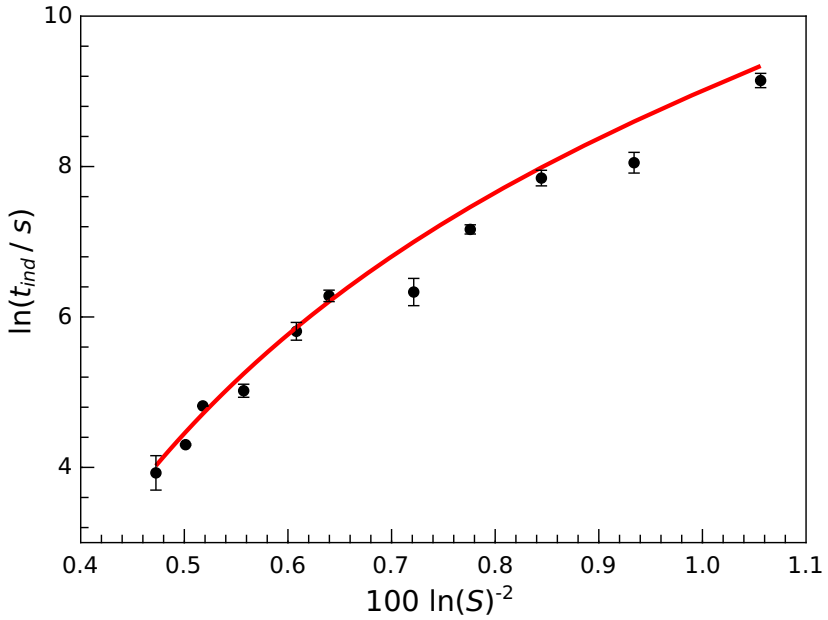

Fig. S1 The dependence of induction time on supersaturation. Also shown with red line is the result of the kinetic model calculations.

D Modeling calculations

In the modeling calculations for room temperature experiments, we adjust parameters of k_i ($i = 1..3$) and k_4 to minimize the weighted sum of residuals (σ) defined as

$$\Sigma = \sum_{i=1}^{n} \frac{(t_{ind,exp} - t_{ind,calc})^2}{\sigma^2}, \tag{S3}$$

where $t_{ind,exp}$ is the experimentally determined induction time, σ is the standard deviation associated with it, and $t_{ind,calc}$ is the induction time calculated from the model. As Fig. (S2) shows, the minima of Σ forms a line in the $\Sigma(k_4, k_i)$ surface along which the parameter sets describe the experimental observation at room temperature equally well. The concentration dependence of induction time does not allow the separation of various parameters sets; the lines with different k_4 values overlap, as Fig. S3 reveals.

The fitting to experimental data including all temperatures deviates along k_4 as the calculated temperature-dependent induction times shows significant difference in k_4 at higher temperatures (see

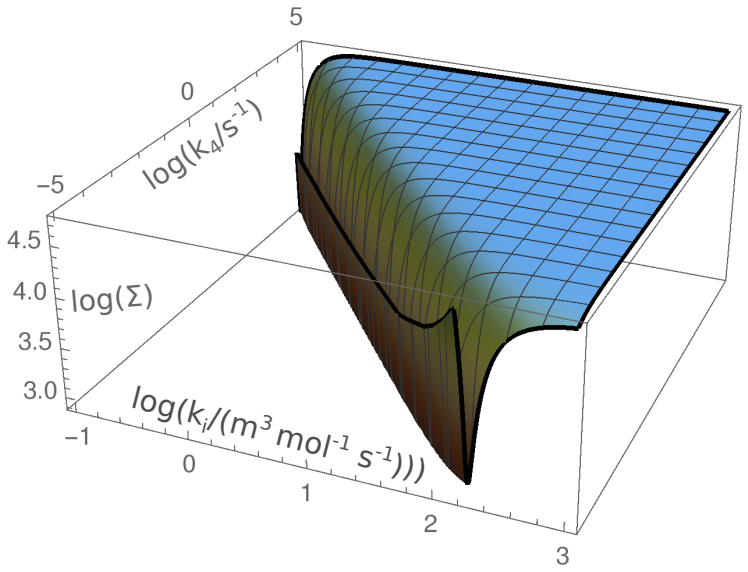

Fig. S2 The weighted sum of residuals (Σ) is characterized by a line in the (k_4, k_i)-plane formed by the minima, where parameters sets describe room temperature measurements equally well.

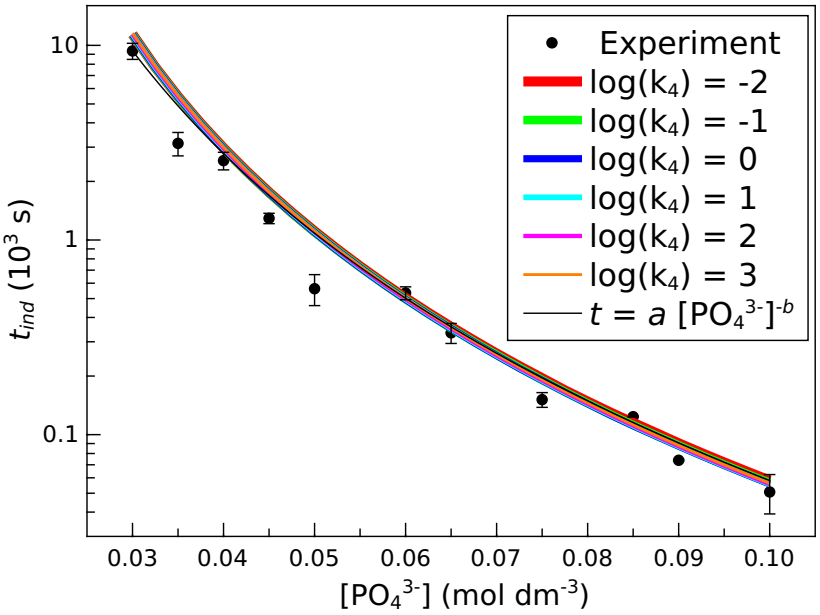

Fig. S3 Induction time as a function of initial phosphate concentration at $T = 25$ °C. The black solid line shows the power-law fitting according to Eqn. (1). The colored lines represent the calculated induction times from the kinetic model based on Eqns. (9)–(13) at various k_4 values.

Fig. S4). The weighted sum of residuals now has a distinct minimum in the $(E_{a,-i}, E_{a,4})$-plane, allowing to provide a good estimate for the appropriate activation energies.

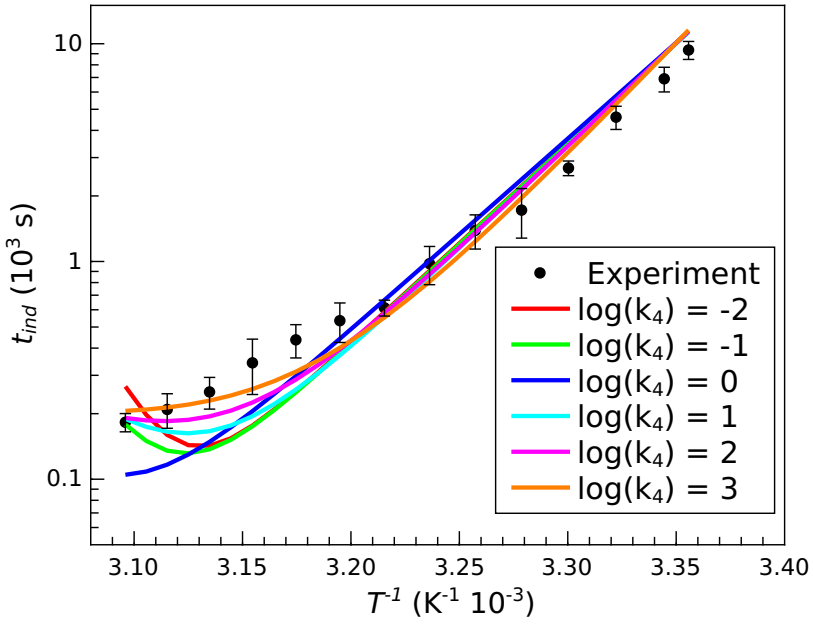

Fig. S4 Temperature dependence of the induction time for stoichiometric composition with $[PO_4^{3-}]_0 = 0.030$ M. The solid lines show the results of modeling for different k_4 values associated with room temperature.

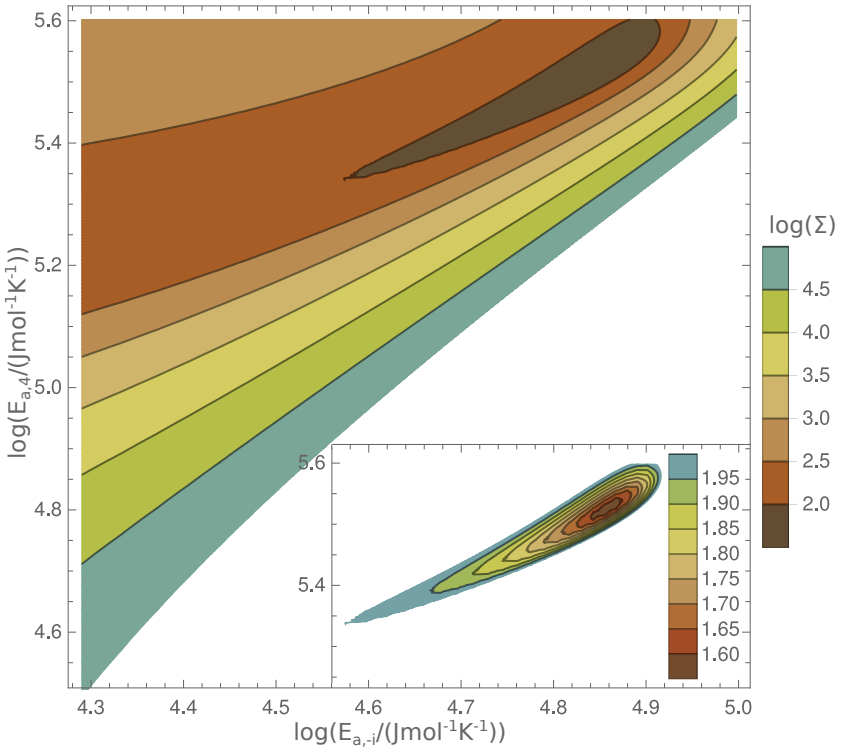

Fig. S5 The weighted sum of residuals (Σ) has a minimum in the $(E_{a,-i}, E_{a,4})$-plane for an example case of $\lg k_4 = 2$ from which experimentally accepted activations energies can be obtained.

The final, suggested rate coefficients are the following:

Table S2 Rate coefficients and activation energies for the model

$k_1 = k_2 = k_3$	$0.296\ \mathrm{M^{-1}s^{-1}}$
$k_{-1} = k_{-2} = k_{-3}$	$10^5\ \mathrm{s^{-1}}$
k_4	10^4
$E_1 = E_2 = E_3$	$19.5\ \mathrm{kJ\,mol^{-1}}$
$E_{-1} = E_{-2} = E_{-3}$	$37.5\ \mathrm{kJ\,mol^{-1}}$
E_4	$250\ \mathrm{kJ\,mol^{-1}}$

E Determination of the polydispersity index

The polydispersity index (PDI) which defines the measure of the heterogeneity of the particle size distribution, was determined from

$$PDI = \left(\frac{\sigma}{2d}\right)^2 \tag{S4}$$

where σ is the standard deviation of the particle size distribution and d is the longer size of the flat-sheet-like particles.

F Determination of crystalline structure

The identification of crystalline Li_3PO_4 is based on the diffractograms in Fig. S6.

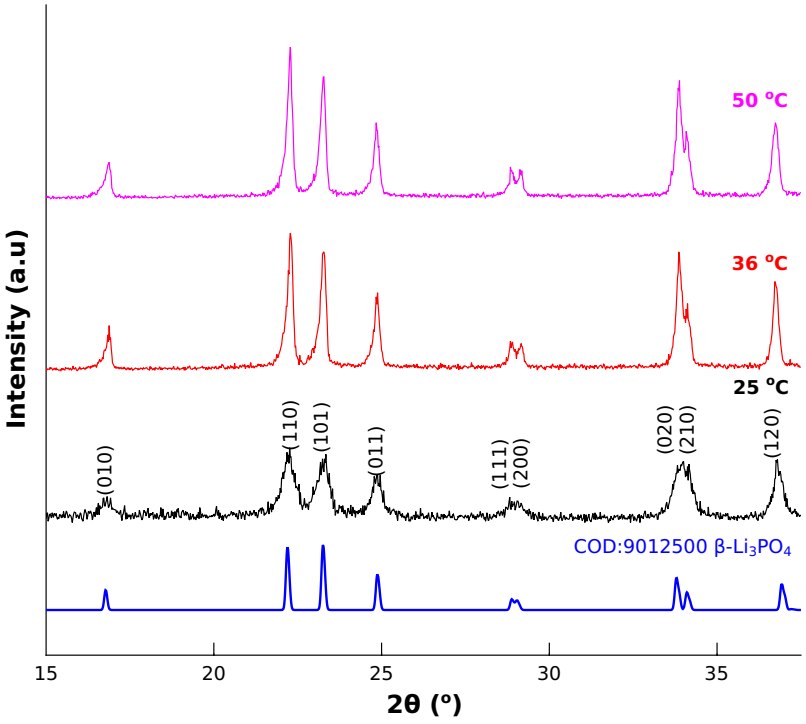

Fig. S6 Diffractograms of the products and the reference $\beta - Li_3PO_4$.

References

1 *Handbook of Chemistry and Physics*, ed. R. C. Weast, CRC Press Inc., Cleveland, 2005.